Renewable and Sustainable Energy Reviews 47 (2015) 448–461

Contents lists available at ScienceDirect

Renewable and Sustainable Energy Reviews

journal homepage: www.elsevier.com/locate/rser

Review of organic Rankine cycle (ORC) architectures for waste heat recovery

Steven Lecompte [a,b,*], Henk Huisseune [a], Martijn van den Broek [a,b], Bruno Vanslambrouck [b], Michel De Paepe [a]

[a] Department of Flow, Heat and Combustion Mechanics, Ghent University – UGent, Sint-Pietersnieuwstraat 41, 9000 Gent, Belgium
[b] Department of Industrial System and Product Design, Ghent University – UGent, Graaf Karel de Goedelaan 5, 8500 Kortrijk, Belgium

ARTICLE INFO

Article history:
Received 17 October 2014
Received in revised form
9 January 2015
Accepted 8 March 2015
Available online 30 March 2015

Keywords:
Organic Rankine cycle
Architectures
Performance evaluation
Waste heat recovery

ABSTRACT

The organic Rankine cycle (ORC) is commonly accepted as a viable technology to convert low temperature heat into electricity. Furthermore, ORCs are designed for unmanned operation with little maintenance. Because of these excellent characteristics, several ORC waste heat recovery plants are already in operation. Although the basic ORC is gradually adopted into industry, the need of increased cost-effectiveness persists. Therefore, a next logical step is the development of new ORC architectures. Even though there has been a strong renaissance towards ORC research in the last decade, ORC architectures have received relatively little attention. Several barriers can be listed. First, there is the difficulty in assessing the additional complexity of the system. While several advanced cycle designs appear promising from a thermodynamic viewpoint, it is not clear that these represent viable economic solutions. Secondly, there is a lack of experimental data from open literature. Additionally, there is the challenge of coping with various boundary conditions from literature, which makes an objective comparison difficult. In this article an overview is presented of ORC architectures. The performance evaluation criteria and boundary conditions are clearly stated. As well, an overview of the available experimental data is given.

Contents

* Corresponding author at: Department of Flow, Heat and Combustion Mechanics, Ghent University – UGent, Sint-Pietersnieuwstraat 41, 9000 Gent, Belgium. Tel.: +32 47004552; fax: +32 92643289.
E-mail addresses: steven.lecompte@ugent.be (S. Lecompte), Martijn.vandenBroek@UGent.be (M. van den Broek), Michel.dePaepe@UGent.be (M. De Paepe).

http://dx.doi.org/10.1016/j.rser.2015.03.089
1364-0321/

1. Introduction

As the human population grows, it becomes increasingly dependent on energy. Especially electricity takes a central role. However, our non-renewable primary energy resources are finite. Furthermore, generation of electricity by burning fossil fuels puts a significant strain on the environment. Therefore it is essential to increase conversion efficiencies to optimally exploit the potential of our resources. This is the landscape where the organic Rankine cycle (ORC) comes into play. Although almost identical to the classical water/steam Rankine cycle, ORC can convert heat at low temperature to electricity due to a careful selection of an alternative working fluid (WF). Further benefits include low maintenance, favorable operating pressures and autonomous operation. Over the last decade the ORC has become a mature technology. Several manufacturers already have a substantial list of reference installations [1,2]. In addition, historical installations [3] have proven the benefits associated to ORCs. While several ORCs are already in operation, the strategic challenge remains of improving the thermodynamic performance and thus also the competitiveness of the ORC.

There are five main focus points when optimizing an ORC: the heat source type, the selection of the working fluid, the hardware components, the control strategy and the component layout and sizing. The heat source can be waste heat, solar energy, geothermal heat or biomass combustion [2]. From a European perspective 2.5 GW [4] of gross electric power could be produced from available waste heat by ORCs. As such, this work main focus is on waste heat recovery applications. Numerous works in literature concentrate on fluid selection, e.g. [5–10]. Initially, fluid selection recommendations were based on simple thermodynamic performance criteria. However, in one of the earliest works about ORCs, Angelino et al. [11] already stipulate the importance of taking technical criteria into account. More recently the working fluid selection takes design and financial appraisal [12,13] into consideration. Screening schemes are set up and multi-objective optimization approaches are introduced [14–18]. Besides the selection of the optimal working fluid, the development of new and improved expander designs gains a lot of attention [19–23]. Another research area which has bloomed is the optimal control strategy of ORCs [24–26]. Finally, the remaining degree of freedom is the choice of cycle architecture and consecutively the sizing of the components. Akin to the classic water/steam Rankine, cycle adaptations such as adding reheaters and recuperators or working in supercritical regime can improve the performance and cost-effectiveness. This development path can also be noted in vapor compression cycles [27]. Therefore exploring cycle adaptations for ORCs is a logical next step. A brief overview of some ORC architectures can already be found in the review article of Tchanche et al. [28] and Ziviani et al. [29].

When compiling an overview of cycle architectures found in literature, it is immediately obvious that diverse boundary conditions and performance criteria are used. This makes a direct comparison difficult. Therefore, in this article, the performance evaluation criteria and boundary conditions are clearly stated. Before we begin the overview, we highlight the potential of advanced cycle architectures for waste heat recovery applications [30].

2. Thermodynamics of waste heat recovery

Typical for waste heat recovery applications are the low temperatures ($< 350\ ^{\circ}C$) and the low heat content. The heat carrier (HC) can be a fluid, steam or flue gasses. In contrast to solar or geothermal (GEO) applications, the heat carrier often forms an open loop. To avoid condensation of acidic flue gasses, a higher cooling limit can be imposed. The dew point temperature depends on the composition of the flue gas, but typical values range from around 100 °C to 130 °C [31–33]. For heat to power applications, the main operational goal is the maximization of the net power output.

The reference technology for converting waste heat to electricity is the subcritical ORC (SCORC). Also sometimes defined in literature as the basic ORC (B). The cycle layout and corresponding T-s diagram of the basic ORC are given in Fig. 1. The basic ORC consists of a pump which pressurizes the working fluid and transports it to the evaporator (1). In the evaporator, the working fluid is heated to the point of saturated or superheated vapor (2). Next, the working fluid expands (3) through an expander and produces mechanical work. This shaft power can then be converted to electricity by the generator. The superheated working fluid at the outlet of the expander is condensed to saturated liquid (4) in the condenser. The liquid working fluid is again pressurized by the pump, closing the cycle. The heat sink and heat source are a finite thermal reservoir and are indicated respectively as line (7)–(8) and (5)–(6).

In the following section, the thermodynamic performance criteria used in literature are briefly discussed. Next, the benefits

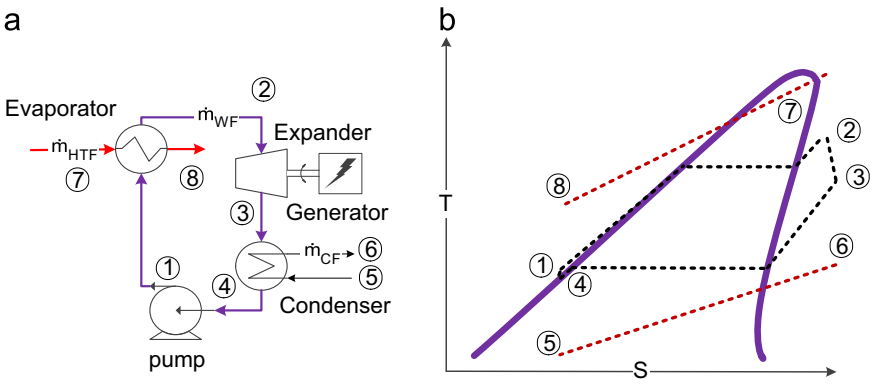

Fig. 1. (a) Subcritical ORC cycle layout. (b) Subcritical ORC T-s diagram.

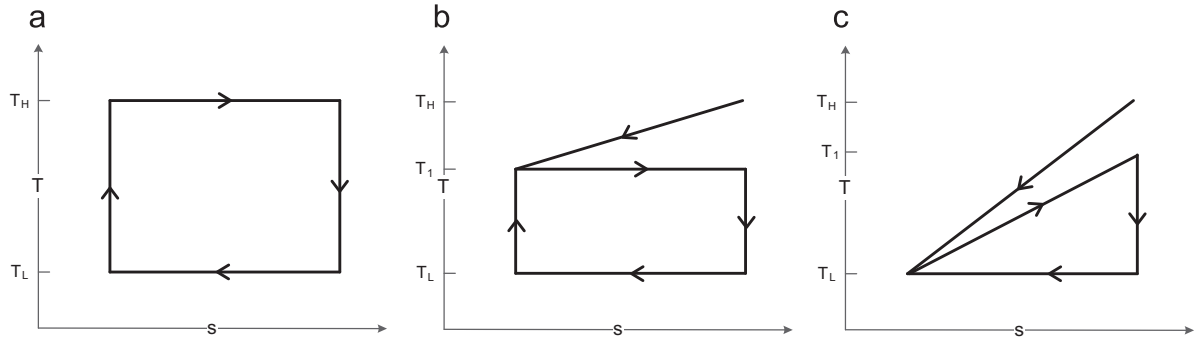

Fig. 2. T-s diagram. (a) Ideal Carnot cycle, infinite capacity heat source. (b) External irreversible Carnot cycle, finite capacity heat source. (c) Ideal triangular cycle, finite capacity heat source.

of new cycle architectures are highlighted by examining the heat recovery process.

2.1. Performance evaluation of thermodynamic cycles

2.1.1. Ideal cycles

In this section, three ideal cycles are analyzed to give insight into the potential of modified ORC architectures and the performance evaluation criteria. The cycles under consideration are the Carnot cycle, the external irreversible Carnot cycle and the ideal trilateral cycle (TLC). A T-s diagram for each of the cycles is given in Fig. 2. For ideal cycles the isentropic efficiency of pump (Eq. 1) and expander (Eq. 2) are equal to one and the heat exchange areas are assumed infinite.

$$\eta_p = \frac{h_{pump,out,isentropic} - h_{pump,in}}{h_{pump,out} - h_{pump,in}} \tag{1}$$

$$\eta_t = \frac{h_{turbine,in} - h_{turbine,out}}{h_{turbine,in} - h_{turbine,out,isentropic}} \tag{2}$$

The thermal efficiency [9,34] can be defined as:

$$\eta_{th} = \frac{\dot{W}_{net}}{\dot{Q}_{in}} = \frac{\dot{W}_{turbine} - \dot{W}_{pump}}{\dot{Q}_{in}}, \tag{3}$$

with $\dot{W}_{turbine}$ the output power at the expander shaft, $\dot{W}_{pump}$ the pumping power and $\dot{Q}_{in}$ the heat flow to the ORC. For a Carnot engine, Fig. 2a, that receives and rejects heat reversibly respectively at T_H and T_L from an infinite thermal reservoir, the thermal efficiency is:

$$\eta_{th,cn} = 1 - \frac{T_L}{T_H} \tag{4}$$

However, this is not representative for waste heat sources. Therefore the situation in Fig. 2b is analyzed; a finite capacity heat source is introduced coupled to a reversible Carnot engine [35]. The fraction of heat recovered from this stream is equal to:

$$\eta_{frac,CN} = \frac{T_H - T_1}{T_H - T_L} \tag{5}$$

The cycle efficiency of this external irreversible Carnot cycle is:

$$\eta_{cycle,CN} = \eta_{frac,CN}.\eta_{th,CN} = \frac{T_H - T_1}{T_H - T_L}.\left(1 - \frac{T_L}{T_1}\right) \tag{6}$$

The maximum power output is found for:

$$T_1 = T^*_{CN} = \sqrt{T_L T_H} \tag{7}$$

which corresponds to a thermal efficiency:

$$\eta^*_{th,CN} 1 - \sqrt{\frac{T_L}{T_H}} \tag{8}$$

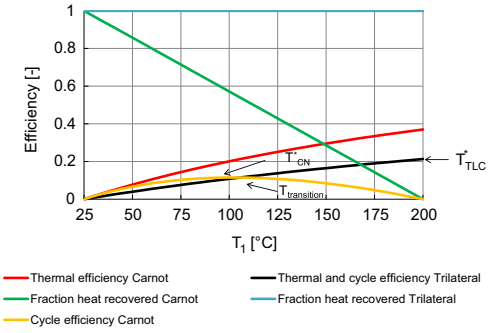

Fig. 3. Thermal efficiency, fraction of heat recovered and cycle efficiency of the Carnot cycle, external irreversible Carnot cycle and TLC in function of the temperature T_1 for T_L=25 °C and T_H=200 °C.

The thermal efficiency at maximum power output is also called the Curzon–Ahlborn efficiency [36]. For a finite capacity heat source the best thermal match with the heat source is made with an ideal triangular cycle as shown in Fig. 2c. Take note that the heat sink is still considered to be an infinite thermal reservoir. The trilateral cycle is further discussed in Section 3.2. The thermal efficiency for the ideal trilateral cycle [37] is given as:

$$\eta_{th,TLC} = 1 - \frac{T_L \ln(T_1/T_L)}{T_1 - T_L} \tag{9}$$

As there is a perfect match with the heat source, the fraction of heat recovery is equal to one and $\eta_{th,TLC} = \eta_{cycle,TLC}$.The maximum power output is found for:

$$T_1 = T^*_{TLC} = T_H \tag{10}$$

In Fig. 3 the above equations are plotted for T_L=25 °C and T_H=200 °C while T_1 varies between 25 °C and 200 °C. It is clear that the thermal efficiency of the trilateral cycle is always lower than that of the Carnot cycle. However, for the TLC both the thermal efficiency and heat recovery increase with T_1, ultimately leading to higher cycle efficiencies. In contrast, for the external irreversible Carnot cycle, the thermal efficiency increases for higher T_1 but the fraction of heat recovered decreases. Thus optimization of the thermal efficiency will not necessarily correspond with optimization of the thermal efficiency [9,38]. The point where $\eta_{cycle,TLC}$is equal to $\eta^*_{th,cn}$ is designated $T_{transition}$ and is linear inT_H. The difference $T^*_{diff} = T_{transition} - T^*_{cn}$ indicates how much higher the working fluid needs to be heated so that the TLC has higher cycle efficiency then the external irreversible Carnot cycle. T^*_{diff} increases from 0.7 °C for T_H=100°C to 3.3 °C for T_H=200 °C and has an almost quadratic behavior. The working fluids in an ideal TLC should therefore not be heated much higher than for a Carnot cycle to see an improvement in cycle efficiency. The benefit

of alternative architectures, considering a more realistic heat recovery process, is further detailed in Section 2.2.

2.1.2. Second law efficiency

According to DiPippo [40] exergy efficiency is the most appropriate indicator to compare thermodynamic performances. This criterion defines how well the incoming heat is converted into power and takes into account the characteristics of the heat source and the environment. The exergy flow rate, or potential work, at a state point i and a mass flow rate $\dot{m}$ is given as:

$$\dot{E}_i = \dot{m}_i.e_i \tag{11}$$

with e_i the specific flow exergy, disregarding the kinetic and potential energy changes:

$$e_i = h_i - h_0 - T_o(s_i - s_0) \tag{12}$$

The subscript 0 refers to the dead state, often chosen as the ambient. A detailed discussion about the fundamental principles of exergy can be found in the work of Kotas [39] and DiPippo [40].

The exergy efficiency is determined by the boundary region of the system. Therefore different forms of exergy efficiency are used in literature. The indices used below refer to Fig. 1. If the waste heat after cooling in the evaporator is unused and only the power at the expander shaft is taken as output, the exergy efficiency is given as:

$$\varepsilon_u = \frac{\dot{W}_{net}}{\dot{E}_7} \tag{13}$$

where E_7 is the exergy of the waste heat source at the inlet of the evaporator:

$$\dot{E}_7 = \dot{m}_{WF}\left[h_7 - h_0 - T_0(s_7 - s_0)\right] \tag{14}$$

In some works ε_u is called the utilization exergy efficiency [40–43]. Quoilin et al. [44] defined the overall energy conversion efficiency as:

$$\eta_{overall} = \frac{\dot{W}_{net}}{\dot{m}_{HC}.cp_{HC}.(T_7 - T_0)} \tag{15}$$

Which closely relates to the exergy efficiency ε_u. The internal exergy efficiency ε_i [41–43,45] discards the absorption of heat available from the heat carrier flow:

$$\varepsilon_i = \frac{W_{net}}{\dot{E}_2 - \dot{E}_1} \tag{16}$$

As a result the internal exergy efficiency only considers how effective the cycle is in converting heat to work. This parameter does not reflect how effective the cycle is in absorbing heat. The external exergy efficiency ε_e [41–43] is similar to the previous definition but accounts for the irreversibility due to heat transfer across a finite temperature difference.

$$\varepsilon_e = \frac{\dot{W}_{net}}{\dot{E}_7 - \dot{E}_8} \tag{17}$$

For some applications, such as combined heat and power (CHP), the waste heat after the ORC is reused. Minimization of the internal irreversibilities is key in optimizing this type of cycle. Therefore the external exergy efficiency is then more appropriate as a performance criterion.

2.2. The ORC heat transfer process

In Section 2.1.1 an infinite heat exchange area was assumed. For real systems however, the heat exchangers are not infinitely large. This results in a minimum temperature difference between the thermal streams. Secondly, with real working fluids, the slopes and shape of the saturation curve primarily influence the heat recovery process. The system can thus be optimized by selecting a proper working fluid and architecture, which is operated at suitable working conditions [5].

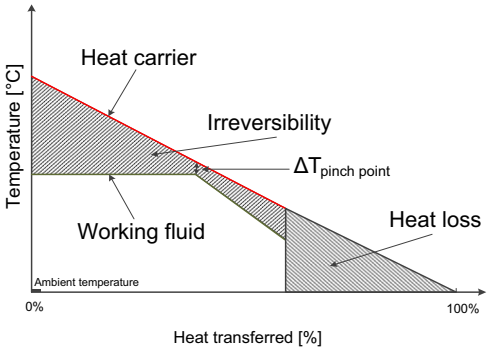

Fig. 4. Temperature–heat diagram for the high temperature side of a subcritical ORC omitting superheating.

By taking these considerations into account, the fundamentals of ORC waste heat recovery can be further explained with the help of Fig. 4. The heat transfer rate in function of temperature is given for an evaporator of a subcritical ORC. The heat transfer rate is expressed in percentage of total heat recovered; with as reference state the ambient. The pinch point temperature difference (PP) is the minimum temperature difference between the two streams. The pinch point limitation, the evaporation temperature and the condensation temperature fix the outlet temperature of the heat carrier and therefore the heat input (Eq. 18).

$$\dot{Q}_{in} = \dot{m}_{HC}.c_{p,HC}.(T_{HC,in} - T_{HC,out}) \tag{18}$$

Two main losses are observed. Firstly, the heat that is still available at the exit of the ORC is usually lost to the environment. This loss is quantified in Eq. (19). The ambient temperature is taken as reference for the lower cooling limit.

$$\dot{Q}_{loss} = \dot{m}_{HC}.c_{p,HC}.(T_{HC,out} - T_{ambient}) \tag{19}$$

Secondly, there are the irreversibilities due to the finite temperature heat transfer. The larger these irreversibilities are, the less potential there is for doing work. Especially for low waste heat temperatures, these have a significant impact on the subcritical heat exchange process [46,47].

Decreasing the exit losses (Eq. 19) to the cycle is done by shifting the pinch point limitation. Decreasing the irreversibilities due to finite temperature heat transfer is accomplished by minimizing the average temperature difference during heat transfers. Thus, matching the temperature profiles of the waste heat carrier and the working fluid. In view of this, a variety of advanced cycle architectures are proposed:

- Transcritical cycles (TC)
- Trilateral cycles (TLC)
- Cycles with zeotropic mixtures as working fluids (ZM)
- Cycles with multiple evaporation pressures (MP)
- Organic flash cycles (OFC)
- Cascade cycles

Increasing the thermal efficiency is achieved by maximizing the mean temperature difference between heat addition and heat rejection. The following cycle modifications have exactly this as main objective:

- Addition of a recuperator (RC)
- Regenerative cycle with turbine bleeding (RG)
- Cycle with reheaters
- Cycle with vapor injector

It is important to realize that all the proposed modifications have an effect on both the heat recovery process and the thermal efficiency. This necessitates a detailed thermodynamic analysis under various boundary conditions and operational regimes.

3. Organic Rankine cycle architectures

In this section, the different cycle architectures are discussed bearing in mind the performance evaluation criteria. First of all, an overview of all the papers is provided in Table 1. From this table it is clear that various boundary conditions are taken for isentropic efficiencies and pinch point temperature differences. Also the heat source temperatures T_7 vary widely between 20 °C and 450 °C. Furthermore, the technical particularities for each of the modified cycles require additional assumptions making a fair comparison difficult.

3.1. ORC with recuperator (RC)

Several authors [9,48] suggest a recuperator to reuse the heat after the expander to preheat the working fluid. The cycle layout and T-s diagram are given in Fig. 5. A recuperator essentially increases the thermal efficiency [9]. Thus a high power output can be maintained for a decreased heat input to the ORC.

Table 1
Overview of papers about advanced ORC architectures and their boundary conditions.

Ref.	T_7 [°C]	T_5 [°C]	Cycle	η_p	η_t	PP_e [°C]	PP_c [°C]	Specific Application	Power scale
[7]	300[a]	30	B	1	1	20	n/a	WHR	n/a
[7]	200[a]	30	B	1	1	20	n/a	WHR	n/a
[9]	100–30	30	B	0.65	0.85	n/a	n/a	GEO	1 MW
[12]	100	15[b]	B	0.80	0.80	[c]	[c]	WHR	7 MWe
[49]	57–240	30[b]	B+RC	0.95	0.85	5	n/a	n/a	100 kWe
[50]	145	25[b]	B+RC	0.60	0.85	8	n/a	WHR	140 kWe
[52]	375–450	30[b]	B+RC	0.80	0.85	n/a	n/a	WHR	100 kWe
[46]	177	25	B+RG	0.80	0.85	n/a	n/a	WHR	n/a
[31]	490		B+RC & B+RG	0.90	0.80	10	10	WHR	n/a
[55]	80–160[d]	10–30	B+RC & B+RG	0.85	0.80	2–10	5	WHR	50 MWe
[54]	120	20	B+RC+RG	0.75	0.85	[c]	[c]	Solar	n/a
[53]	80–213[a]	40–50[b]	B+RC+RG	0.65	0.80	10	10	WHR	50–3300 kWe
[41]	300	30	B & OFC & TC & ZM	0.85	0.85	10	10	n/a	n/a
[58]	300	30	OFC modifications	0.85	0.85	10	10	n/a	n/a
[59]	90–140	40	B & OFC	n/a	n/a	10	10	GEO	n/a
[59]	90–140	40	B & OFC	n/a	n/a	5	5	GEO	n/a
[60]	30–200[d]	30[b]	B & TLC & TC	0.6	0.75	n/a	n/a	n/a	n/a
[64]	63–350	15–150	B+RC & TC+RC & TLC+RC	0.65	0.85	10	10	n/a	n/a
[62]	150–350	15–62	B & TLC & TC	0.65	0.85	10	10	n/a	n/a
[65]	150	25	B & TLC+ZM	1.00	0.70	n/a	n/a	n/a	n/a
[72]	120	15	B+RC & ZM+RC	0.75	0.80	5	5	GEO	n/a
[74]	85[d]	25[b]	B+RC & ZM+RC	1.00	0.80	n/a	n/a	Solar	n/a
[71]	140	12	B+RC & ZM+RC	0.50	0.75	10	n/a	GEO	n/a
[73]	150	25	B+RC & ZM+RC	0.80	0.65	20	10	WHR	200–300 kWe
[73]	250	35	B+RC & ZM+RC	0.80	0.65	30	20	WHR	200–300 kWe
[51]	177	42[b]	B+RC & ZM+RC	1.00	0.85	[c]	n/a	WHR	50 kWe
[42]	150	20	B+RC & ZM+RC	0.60	0.75	10	10	WHR	n/a
[92]	80–200	15	B & MP & TC & ZM	n/a	n/a	10	10	n/a	n/a
[92]	80–200	15	B & MP & TC & ZM	n/a	n/a	2.8	2.8	n/a	n/a
[71]	350	50	B+RC & ZM & TC+ZM+RC	0.50	0.75	10	n/a	WHR	n/a
[81]	100	20	TC	0.80	0.80	[c]	[c]	n/a	300 We
[84]	220	n/a	TC	n/a	n/a	10	n/a	n/a	n/a
[82]	120–180	15	B+RC & TC+RC	0.70	0.85	[c]	[c]	GEO	n/a
[6]	250[d]	85[b]	B+RC & TC+RC	0.65	0.85	n/a	n/a	CHP	1 MWe
[6]	250[d]	38[b]	B+RC & TC+RC	0.65	0.85	n/a	n/a	WHR	1 MWe
[6]	300[d]	85[b]	B+RC & TC+RC	0.65	0.85	n/a	n/a	CHP	1 MWe
[6]	280	85[b]	B+RC & TC+RC	0.65	0.85	10	n/a	CHP	1 MWe
[6]	350	85[b]	B+RC & TC+RC	0.65	0.85	10	n/a	CHP	1 MWe
[32]	300	10	B+RC & TC+RC	0.75	0.75	10	10	WHR	n/a
[32]	300	70	B+RC & TC+RC	0.75	0.75	10	10	CHP	n/a
[32]	170	10	B+RC & TC+RC	0.75	0.75	10	10	GEO	n/a
[32]	100	10	B+RC & TC+RC	0.75	0.75	10	10	GEO	n/a
[61]	210	20[b]	B & TC	0.85	0.8	10	10	n/a	n/a
[47]	90	20	B & TC	0.75	0.8	5	5	GEO	5–10 kWe
[83]	130–170	20–35[b]	B & TC	0.8	0.8	20	20	GEO	n/a
[90]	120	20	MP	1	1	n/a	n/a	n/a	n/a
[87]	163	13	MP level I	0.8	0.666	7.9	n/a	GEO	1.219 MWe
[87]	163	13	MP level II	0.8	0.708	2.9	n/a	GEO	0.940 MWe
[91]	110–160	30–40[b]	B & MP & TC	0.85	0.85	7–10	7–10	GEO	1 MWe
[31]	490	15	B+TC & MP	0.9	0.80	10	10	WHR	n/a
[93]	147	35[b]	B+injector	1	1	n/a	n/a	n/a	n/a
[94]	304	26.7	B+RC+reheater	0.67	0.75	9.4	7.2	Solar	1 MWe
[95]	130–140[a]	35	B+cascade	n/a	n/a	n/a	n/a	Solar	n/a

[a] Saturation evaporation temperature is given instead of T_7.
[b] Saturation condensation temperature is given instead of T_5.
[c] Detailed heat transfer model.
[d] Expander inlet temperature T_2 is given instead of T_7.

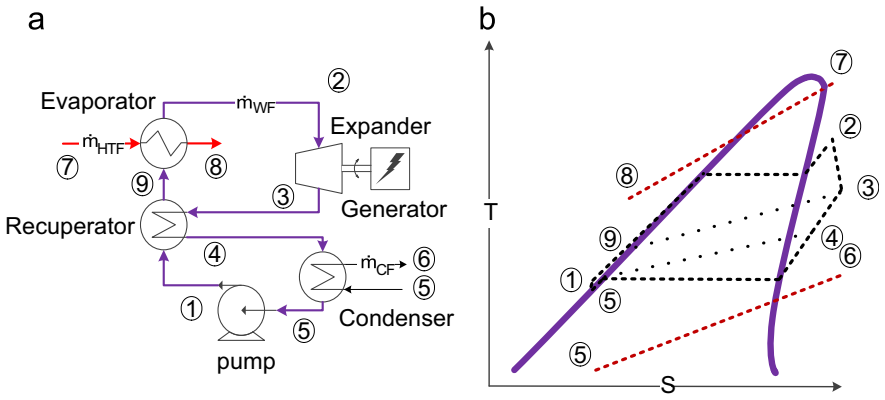

Fig. 5. (a) ORC with recuperator cycle layout. (b) ORC with recuperator T-s diagram.

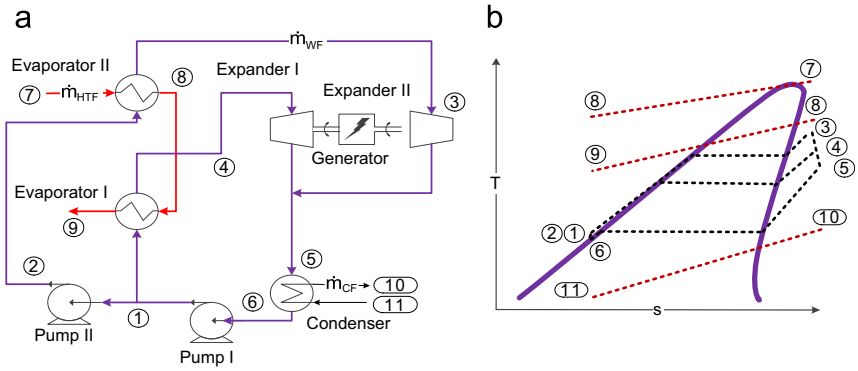

Fig. 6. (a) ORC with turbine bleeding cycle layout. (b) ORC with turbine bleeding T-s diagram.

In order to implement a recuperator, a superheated state is necessary after the expander. In the case of dry fluids [5,7,49] a strongly superheated vapor exits the expander. This increases the load on the condenser. However, if there is no limitation on the temperature to which the flue gasses can be cooled, the net power output will not increase by adding a recuperator [32,50]. The net work output will approximately be the same. Furthermore, in the cited studies the increased pressure drop and the extra cost of the recuperator are neglected.

A recuperator can be beneficial [6,50,51] for waste heat recovery applications, if there is a higher cooling limit of the heat carrier. When flue gasses containing water and sulfur trioxide are cooled below the acid dew point, sulfuric acid vapor condenses. These acids potentially lead to corrosion and damage of the heat exchanger and should be avoided. The temperature of the acid dew point varies with the composition of the flue gas. Typical values range from around 100 °C to 130 °C [31–33].

3.2. Regenerative ORC (RG)

ORCs with turbine bleeding, coupled to a direct contact heat exchanger, are typically designated as regenerative ORCs. These cycles closely resemble the ORC with recuperator, as both pre-heat the working fluid before entering the evaporator. The schematic of the cycle and T-s diagram are shown respectively in Fig. 6a and b. Mago et al. [52] present an analysis of a regenerative ORC and compared this with the basic ORC. Their results show that regenerative ORCs have a higher thermal efficiency and lower irreversibilities. Furthermore, the authors note that the increase in thermal efficiency between cycle types depends strongly on the working fluid used. For some fluids (R245ca) the difference between the two cycle configurations is negligible.

A cycle with both turbine bleeding and recuperator was analyzed by Desai et al. [53]. On average, an relative improvement of 16.5% in thermal efficiency is obtained when compared to the basic ORC cycle. Combining both modifications always gives a better thermal efficiency than the stand alone implementation of turbine bleeding or recuperation.

Pei et al. [54] analyzed a regenerative ORC for use in conjunction with low temperature solar heat. There is an optimal regenerative temperature at which the ORC reaches maximum thermal efficiency. The maximum thermal efficiency is 9.2% higher than the thermal efficiency of the ORC without modifications.

Meinel et al. [31] compared the basic ORC, the ORC with RC and the ORC with turbine bleeding. They too affirm the thermal efficiency gain compared to the basic ORC. Furthermore, for isentropic fluids the ORC with RG has a higher efficiency then that of the basic ORC and the ORC with RC. While for dry fluids the ORC with RC has a higher thermal efficiency then both the basic ORC and ORC with RG. Also Yari and Mahmoudi [55] compared the performance of the basic ORC, the ORC with RC and an ORC with RG. The application was waste heat recovery, with no constraint on the possible condensation of flue gasses. Therefore maximization of the output power is crucial, not maximization of the thermal efficiency. By using a recuperator or turbine bleeding less heat can be transferred to the cycle. As a result, the basic ORC was indicated as the best cycle design in both economic and thermodynamic perspective. The regenerative cycle was found to have potential for cogeneration purposes.

3.3. Organic flash cycle (OFC)

The organic flash cycle (OFC) has its origin in geothermal energy generation [56]. There, liquid brine from a geothermal well is throttled down to a lower pressure in a flash tank. The vapor

fraction is fed to the turbine, the liquid phase is directly returned to the condenser. In order to increase the mass flow rate of vapor, several flash tanks can be connected in series. The liquid brine is mostly composed of water. However, the disadvantage of using the wet steam directly, is the significant amount of moisture that exits the expander [41]. An isentropic expansion of a wet fluid from the saturated vapor state inevitable ends in the two-phase state. Therefore special wet steam turbines are necessary with reinforced material to protect the turbine blades from erosion [56]. This in turn results in an increased production cost. Furthermore, it is known that the turbine isentropic efficiency reduces [57] with the moisture content.

In the OFC, Fig. 7, the liquid brine is not directly flashed, but is fed to a heat exchanger to heat an organic working fluid. In the heat exchanger, boiling of the working fluid is avoided, resulting in a better match between the temperature profiles of the heat carrier and the working fluid. This type of cycle is extensively discussed by Ho et al. [41,58].

In a first paper Ho et al. [41] analyzed the performance of the basic OFC and compared the results to the transcritical cycle, and a cycle with zeotropic mixture. The waste heat has a temperature of 300 °C. The results of this study indicate that the total output power for the OFC is slightly lower in comparison to an optimized ORC for the same conditions of the heat carrier. Still, the OFC captures more heat from the heat carrier compared to other investigated cycles. Because of the low thermal efficiency, this heat is not converted in more mechanical power. The thermal efficiency is low as a result of the irreversibility introduced by the throttling valve. The optimized ORC has the highest power output, followed by the OFC, the transcritical CO_2 cycle and the ORC with zeotropic mixtures. It should be stressed however, that only an ammonia/water mixture was included in the study.

In a second study [58] about the OFC the authors proposed and analyzed enhancements to the OFC to increase power production. These modifications were: double flash OFC, two-phase OFC, modified OFC, two-phase OFC combined with a modified OFC. In the two-phase OFC the throttling valve is replaced by a two-phase expander. In this way the irreversibilities associated with the throttling valve are eliminated. In the double flash system, the working fluid is flashed in two stages and fed respectively to a high and low pressure expander. Because the working fluid is expanded at different pressure levels more vapor is available to produce work. The modified OFC also introduces a high and low pressure expander. Instead of flashing the working fluid at two different pressure levels, the superheated vapor after the high pressure expander is combined with the liquid coming from the flash tank. The resulting saturated vapor at intermediate pressure is then fed to a low pressure expander. There is 5–20% more power output when using the proposed enhancements in comparison to the optimized ORC with hydrocarbons as working fluid. When using siloxanes, there is only a 2–4% increase. This is explained by the authors as caused by the smaller difference in specific entropy between saturated liquid and saturated vapor for siloxanes. This reduces the exergy destruction during isenthalpic throttling. Therefore, the overall effect of modifications to reduce exergy losses is small for siloxanes. Furthermore siloxanes are very dry fluids; hence the majority of exergy destruction is located in the condenser.

A different type of OFC was investigated by Edrisi and Michaelides [59] and is shown in Fig. 8. The working fluid in the investigated cycle evaporates to a certain dryness factor. After partial evaporation the vapor part is separated from the liquid and fed to the expander. The liquid part is flashed and the additionally produced vapor is again fed to an expander. The liquid after

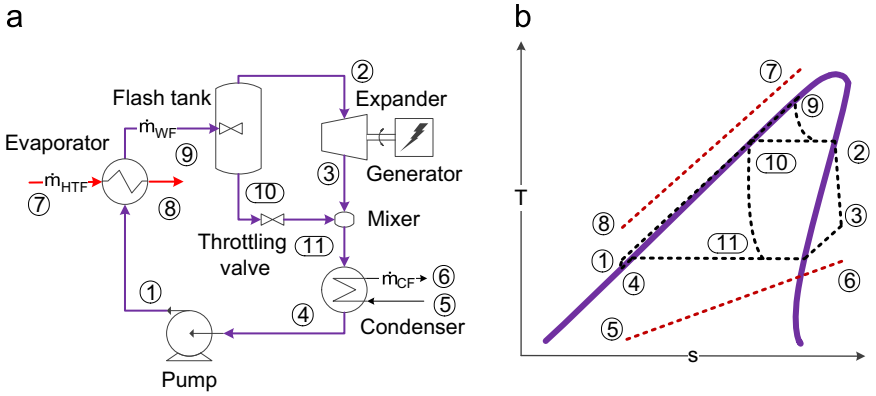

Fig. 7. (a) OFC cycle layout. (b) OFC T-s diagram.

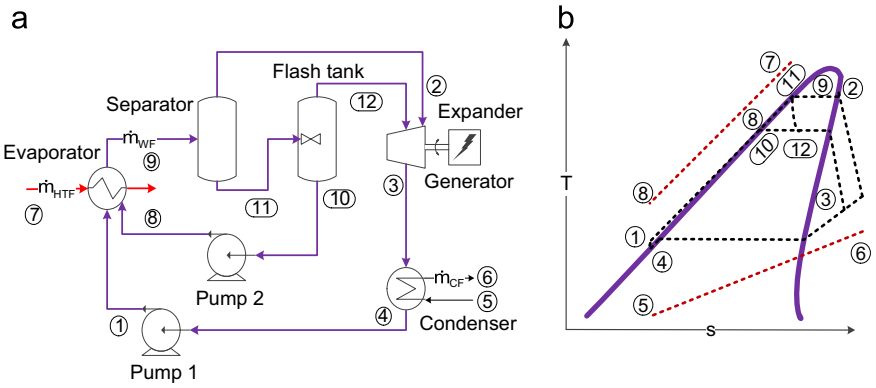

Fig. 8. (a) Alternative OFC system cycle layout. (b) Alternative OFC system T-s diagram.

flashing goes directly to the heat exchanger for partial evaporation. The authors note that practical implementations of this cycle may require an extra expander and heat exchanger. The performance of the cycle is investigated for a heat carrier inlet temperature between 90 °C and 160 °C. The vapor quality and the evaporation temperature are optimized in order to maximize the power output. For the basic ORC, with saturated vapor at the inlet of the expander, only the evaporation temperature is optimized. The results indicate that the outlet temperatures of the heat carrier are significantly lower for the OFC than for the basic ORC. Therefore more heat is absorbed in the OFC to produce work. The optimum dryness factor increases with temperature but is significantly lower than 1. The output power for this type of OFC can be up to 25% higher compared to the basic ORC.

3.4. Trilateral (triangular) cycle (TLC)

The T-s-diagram of the trilateral cycle (TLC), Fig. 9, closely resembles that of the OFC. Instead of flashing the working fluid to produce saturated vapor and saturated liquid, the working fluid is directly fed to the expander. Boiling of the working fluid is avoided in order to shift the pinch point limitation. Intrinsically the TLC has a lower thermal efficiency than the basic ORC [60]. Nevertheless, there is a higher potential to recover heat because of the better match between the temperature profiles of the heat carrier and the working fluid. The combined effect results in a better cycle efficiency. This was discussed in Section 2.1.1 and illustrated in Fig. 3. According to Schuster et al. [61] this match could best be realized with a transcritical cycle instead of a TLC. The results from the work of Fischer et al. [62] however showed that a TLC always has a better performance than the transcritical cycle. Yet, the challenge of triangular cycles is the availability of two-phase expander technology with high isentropic efficiency. According to DiPippo [63] isentropic efficiencies of at least 75% are necessary before adoption in geothermal plants is feasible.

Fischer et al. [62] compared the performance of the TLC to sub- and transcritical ORCs. The working fluid for the TLC is water. For the sub- and transcritical ORCs the working fluid was cyclopentane ($T_7 = 250$–350 °C), n-butane ($T_7 = 220$ °C) or propane ($T_7 = 150$ °C). The cycles are optimized for maximum power output. The exergy efficiency of the TLC is always higher than that of the sub- and transcritical ORC. For $T_7 = 350$ to 220 °C the exergy efficiency is by 14% to 20% higher, while for $T_7 = 150$ °C it is even 29% higher. Furthermore the impact of the volume flow rate is discussed by the authors. The outgoing volume flows from the expander are a factor 2.8 higher for a TLC than for the ORC ($T_7 = 280$ °C, $T_5 = 85$ °C). If T_7 and T_5 are lowered to 150 °C and 38 °C respectively, this becomes a factor 70. The ratio of inlet to outlet volume flow rate over the expander is 100 to 1000 times larger than for the ORC depending on the temperature T_5. The large volume flows are accounted to the low vapor pressure of water at ambient temperatures. Therefore the authors suggest using other working fluids than water for the TLC. In a subsequent study, Lai and Fischer [64] investigate Power Flash Cycles (PFC) with aromates, siloxanes, and alkanes as working fluids. The PFC is considered a generalization of the TLC, also expansion into the superheated region is allowed. According to the authors, cyclopentane is to be preferred in a PFC because of the significantly smaller outlet volume flows then water while achieving a comparable high power production.

The TLC and OFC are developed to improve heat transfer from the waste heat carrier. A next step can be the improvement of heat rejection at the condenser side. By incorporating a zeotropic mixture in the cycle a better match between working fluid and heat sink is possible. Zamfirescu and Dincer [65] analyzed this idea for an

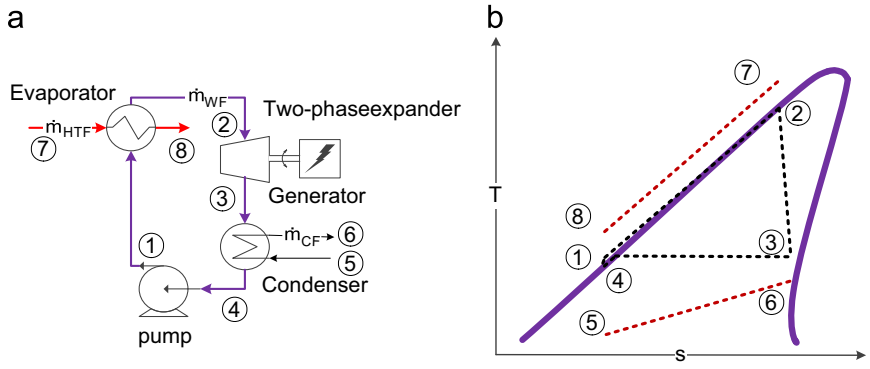

Fig. 9. (a) TLC cycle layout. (b) TLC T-s diagram.

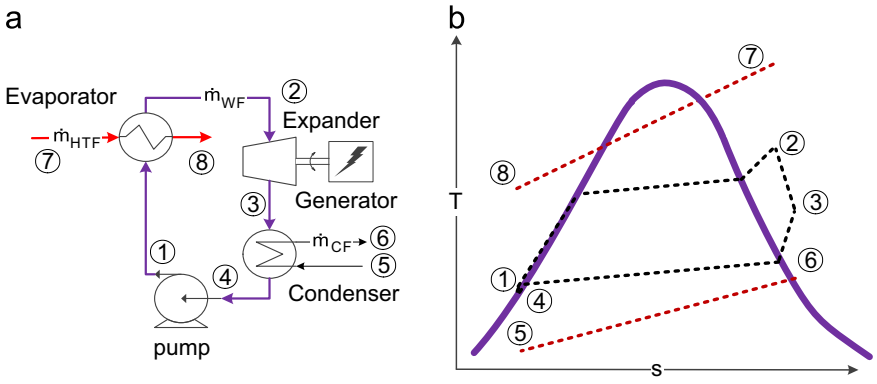

Fig. 10. (a) ORC with zeotropic mixtures cycle layout. (b) ORC with zeotropic mixtures T-s diagram.

ammonia-water trilateral cycle. However, Fischer et al. [62] noted that the advantage of a better temperature glide is small compared to the disadvantage of the corrosive behavior of ammonia.

3.5. Zeotropic mixtures as ORC working fluids (ZM)

A different way of reducing irreversibilities associated to non-isothermal heat addition is the use of zeotropic mixtures. The general plant layout stays the same and is shown in Fig. 10a The non-isothermal phase change of these mixtures, shown in the T-s diagram of Fig. 10b, permits a good match of the temperature profiles in the condenser and evaporator. Furthermore, zeotropic mixtures are already used in cryogenic refrigeration [46].

One of the earliest power cycle designs with a zeotropic mixture was the Kalina cycle [66]. The circuit of the Kalina cycle is different from the ORCs, because the mixture is only present in the heat exchangers and not in the expander. Therefore a separator and absorber are included in the cycle design. The working fluid used in the Kalina cycle is NH_3-water. Lu et al. [67] assessed the performance of the Kalina cycle in comparison to an optimized ORC. They concluded that for low power and medium to high temperature the gains in overall efficiency are very small and this is obtained with a complicated plant layout, high maximum pressures, large surface heat exchangers and non-corrosive materials. Nonetheless, this cycle is commercially available and patented [68]. Besides NH_3-water other organic mixtures are investigated in literature.

From 1990 onwards there were crucial advances in predicting mixture thermodynamic properties. One of the key developments was the design of new computational methods. Colonna [69] made a survey of available methods for the estimation of mixture thermodynamic properties. A computer calculation (StanMix) based on the model by Wong and Sandler [70] was developed. This laid the base for further simulation and analysis of zeotropic mixtures in organic Rankine cycles. Furthermore Angelino et al. [71] analyzed an organic Rankine cycle with a zeotropic mixture of n-butane and n-hexane (50%/50%). The results showed that in particular air cooled condensers or cogeneration benefit from matching condensation temperatures (25% less air is needed). Two concerns are mentioned. The first is the prevention of fluid fraction during phase change in the heat exchangers. The second is the lack of information about heat transfer coefficients when using mixtures.

Heberle et al. [72] investigated the exergy efficiency for zeotropic mixtures of isobutene-isopentane and R227ea-R245fa. For temperatures below 120 °C the exergy efficiency increased relatively with 4.3–15% compared to using pure working fluids. The optimal exergy efficiency was found for the mixture concentration that results in matching temperature glide between working fluid and cooling water.

Chys et al. [73] investigated zeotropix mixtures based on hydrocarbons and siloxanes as working fluids in ORCs. An increase in thermal efficiency of 15.7% and an increase in generated electricity of 12.3% was found for a temperature source of 150 °C. When using a higher temperature source of 250 °C the values decreased to 6.0% and 5.5% respectively. The influence of a third mixture component was analyzed and considered to have a marginal effect.

Wang and Zhao [74] investigated mixtures composed out of R245fa-R152a. As in the work of Heberle et al. [72], the volume flow rate and inlet/outlet volume flow ratio over the expander is decreased when using mixtures. Meanwhile the thermal efficiency is reduced, this is in contrast with the general trend observed [42,72,73]. This is explained by the chosen boundary conditions. The lowest and highest temperature of the cycle were fixed. Therefore the ability to match the temperature profile to an external heat carrier (evaporator) or cooling loop (condenser) is lost.

Lecompte et al. [42] provided an exergy analysis on ORCs with zeotropic mixtures as working fluids (R245fa-pentane, R245fa-R365mfc, isopentane–isohexane, isopentane–cyclohexane, isopentane–isohexane, isobutene–isopentane and pentane–hexane). The heat carrier inlet temperature T_7 was 150 °C. Using mixtures resulted in an improvement of the exergy efficiency between 7.1% and 14.2% compared to pure working fluids. The source of this improvement is mainly ascribed to decreased irreversibilities in the condenser. This confirms the findings of Heberle et al. [72]. Exergy losses in the condenser are reduced by matching the glide slope of the working fluid with the glide slope of the cooling fluid. Consequently, an optimal mixture concentration exists which maximizes the second law efficiency. The optimal condensing glide slope is however slightly smaller than the glide slope of the cooling fluid due to the exergy losses in the pump, expander and evaporator. The difference between the various optimized ORCs with zeotropic mixtures as working fluid is less than 3 percentage points. Therefore, thermo-economic criteria should be included when ranking working fluids.

3.6. Transcritical cycle (TC)

When looking at the history of steam/water Rankine cycles and refrigeration cycles the logical next step is incorporating a supercritical state. Starting from the 1950s, the first attempts to develop turbine power units based on supercritical states were made. As early as 1957 the first transcritical Rankine cycle was started up in the electric power station of Philo, USA [75]. In the USA alone 159 new transcritical power plants were started up between 1960 and 1990. Furthermore, from the 1990s onwards there is a revival on the study of transcritical refrigeration [76] and heat pump cycles [77]. The importance of the supercritical cycles is further reflected by the more than 1000 patents on this subject.

The major difference between a subcritical and a supercritical organic Rankine cycle lies in the heating process of the working fluid. The cycle layout is identical to that of the basic cycle of Fig. 1, the T-s diagram is shown in Fig. 11. Working fluids are compressed directly to supercritical pressure and heated to the supercritical state, effectively bypassing the two-phase region. By bypassing the isothermal boiling process, the temperature-glide of the transcritical Rankine cycle provides a good thermal match between working fluid and heat source [61]. Thus heat transfer is done more effectively compared to the basic ORC [9].

In a transcritical power cycle, the liquid to vapor phase transition is performed at supercritical pressure, while condensation takes place in the usual two-phase region. In contrast, for a pure supercritical cycle both condensation and evaporation occur in the supercritical state. Note that the difference between supercritical and transcritical is not always used rigorously. For example the classic transcritical water/steam power cycle is often called supercritical. The thermodynamic performance benefits of a transcritical cycle were investigated by among others Angelino and Colonna [71], Saleh et al. [9] and Schuster et al. [61].

Schuster et al. [61] state that for the transcritical cycle an improved power output of 8% is possible compared to the basic subcritical cycle. The thermal efficiency is however lower than that of the basic ORC in favor of an increased heat addition to the cycle, in analogous to the TLC discussed in Section 3.3.

A high power output of the system is linked with the choice of an appropriate organic medium. One of the first working fluids used in supercritical cycles was CO_2 [78–80]. Because of the low critical temperature (31 °C) a supercritical state is easily achieved. Further desirable qualities are the small environmental impact and the low cost. However, because of the high critical pressure (73.8 bar) component costs are high and safety regulations are severe. Therefore also other working fluids are considered. A comparison between a transcritical cycle with working fluid R125 and CO_2 shows an increased power output of 14% for R125 [81]. Even though the carbon dioxide cycle shows better heat transfer and pressure drop characteristics, the high pumping power required to manage the large pressure head degrades the cycle's power output. For this study, the total heat

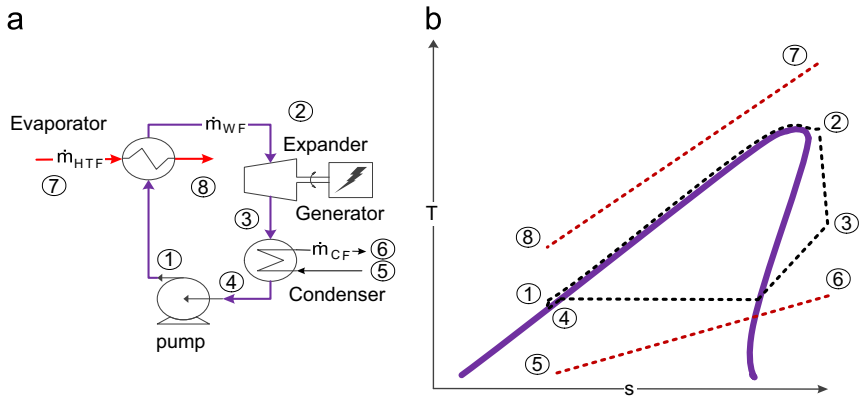

Fig. 11. (a) Supercritical cycle layout. (b) Supercritical T-s diagram.

Table 2
Techno-economic analysis of transcritical cycles in open literature.

Ref.	Performance criteria	Conclusion
[82]	Plant total specific cost (€/kWe)	TC is in comparison to the SCORC the most cost effective solution under sufficient heat carrier temperature drop
[47]	Levelized energy cost [$/kWh] and Heat exchange area per unit power [m²/kWe]	TC with R125 provides the most cost effective solution in comparison with SCORC
[12]	Total specific cost of equipment (€/kWe)	TC with R125 most cost effective compared to TC with CO_2 and ethane

transfer area was fixed. The supercritical cycle with R125 was recommended for heat sources of about 100 °C [47,81].

Astolfi et al. [82] compared the subcritical and transcritical ORC for the exploitation of medium to low temperature geothermal sources. They state that, as a general trend, the configurations based on supercritical cycles employing fluids with a critical temperature slightly lower than the temperature of the geothermal source lead to the lowest electricity cost for most of the investigated cases. Vetter et al. [83] quantify that for optimal power output the working fluid should have a critical temperature of 0.8 times the heat source temperature.

Karellas et al. [84] studied the design of plate heat exchangers for transcritical ORCs based on theoretical models. A calculation and dimensioning method was proposed by discretizing the heat exchanger in various segments and employing the Jackson correlation [85] to calculate the convective heat transfer coefficient in the supercritical region. Their results show that the performance of the TC is higher than the basic ORC without a disproportioned rise of installation costs due to larger heat exchangers. However, they conclude that a techno-economic investigation of real-scale transcritical ORCs is vital before drawing final conclusions. Still, techno-economic studies on transcritical cycles are scarce and diverse performance evaluation criteria are used. A non-exhaustive list is given in Table 2.

3.7. ORC with multiple evaporation pressures (MP)

Another way to decrease the irreversibilities involved in heat transfer over a finite temperature difference is to split the Rankine cycle in different pressure levels [86]. When introducing a second pressure level a new pinch point is created. It is clear from Fig. 12 that for the low pressure loop the exhaust temperature of the heat carrier is lower. Therefore more heat is transferred into the cycle. There is a good match between the high temperature side of the heat carrier and the high pressure loop. Thus a high thermal efficiency can be achieved. The same principle is valid for the low temperature side of the heat carrier and the low pressure loop. The dissipative loss in the evaporators for dual pressure ORCs accounts for 26% of the total irreversibilities [87]. This is relatively low compared to the values for a basic ORC in the work of Mago et al. [46], between 40.4% and 77%, and Shengjun et al. [47], between 30% and 51%.

A careful selection of the pressure levels allows for a maximum exergy transfer. Stijepovic et al. [88] propose a methodology for the design of optimum multi-pressure organic Rankine cycle processes. By increasing the number of pressure levels the cycle approaches the theoretical Lorentz cycle. Lee and Kim [89] showed that for an finite thermal reservoir the maximum work output for the Lorentz cycle is twice that of the Carnot cycle for a given pinch point. However, a lower mean temperature difference between the two streams means that a larger heat transfer area is needed for a given heat transfer rate.

Multi-pressure organic Rankine plants are not analyzed extensively in the open literature. Gnutek and Bryszewska-Mazurek [90] proposed a multi-pressure ORC with R123 as working fluid and a multi-segment sliding-vane expansion machine. Franco and Villani [91] analyzed the basic ORC, TC and MP for geothermal applications. The authors conclude that there is no single optimal working fluid/cycle combination. In some cases advanced cycle designs lead to higher performance, but not always. Only 6 working fluids were investigated: R134a, R152a, isobutene, n-pentane, R410A, R407C. Becquin and Freund [92] investigated several advanced power cycles for waste heat recovery: dual-pressure, transcritical and cycles with ammonia/water mixtures. The working fluids under consideration are: R125, R134a, isobutane and R245fa. The heat source temperature ranged from 80 °C to 200 °C and the cycles are optimized to produce the maximum net power output. Especially at the lower temperatures the modified cycles proved to significantly increase output power (up to 35%). The dual-pressure cycle was the only cycle which offered an increased power output over the whole range of heat source temperatures. Especially for the supercritical cycle and the cycle with zeotropic mixtures the working fluid should ideally be custom-tailored to the cycle design. For the dual-pressure cycle the required total UA (heat transfer coefficient (U) multiplied by heat transfer area (A)) is marginally higher than for the basic ORC. Meanwhile the net power output at a heat source inlet temperature of 100 °C is around 25% higher. The disadvantage lies in the complex layout with dual expanders and two pumps. In general the increased

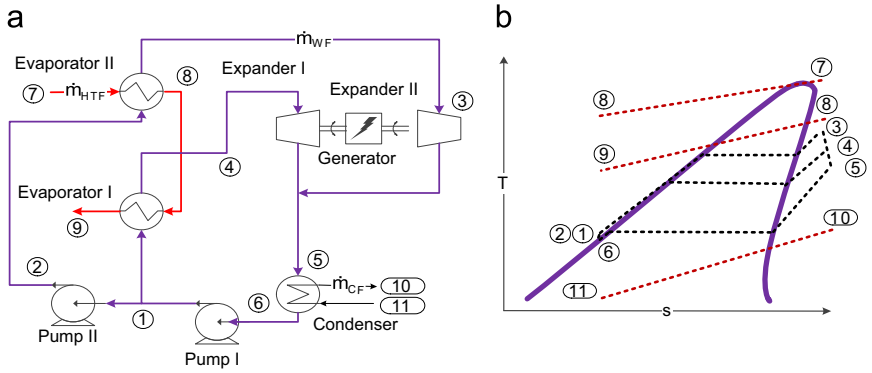

Fig. 12. (a) Multiple evaporation pressure ORC cycle layout. (b) Multiple evaporation pressure ORC T-s diagram.

Table 3
Overview of challenges related to advanced ORC architectures.

Cycle	Modifications	Challenges
B+RC	Extra heat exchanger	Only beneficial if lower cooling limit of flue gasses
B+RG	Multi-stage expander, extra heat exchanger and pump	Only beneficial if lower cooling limit of flue gasses Development of multi stage expanders
OFC	Added flash tank, throttling valve, mixer (other extensions are possible: two-phase expander, multiple flash tanks, multiple expanders)	Performance simple OFC equals basic ORC Many extra components needed
TLC	Two-phase expander	Availability of high efficiency two-phase expanders
MP	Multiple expanders, pumps and heat exchangers	Many extra components needed
TC	Supercritical fluids	High pressures Stability working fluids Limited knowledge about heat exchange and pressure drop correlations for supercritical fluids
ZM	Zeotropic mixtures	No practical experience Limited knowledge about heat exchange and pressure drop correlations for zeotropic mixtures Risk of fluid fraction

power output of the modified cycles is at the expense of a more complicated design and increased heat exchanger surface area.

3.8. Vapor injector, reheater and cascade cycles

In the open literature some other, less investigated, architecture modifications are mentioned. These are shortly presented in this section.

A cycle with a vapor injector as regenerator is proposed by Xu and He [93]. The working fluid used was R123. The cycle consists of the basic ORC components, with the addition of turbine bleeding and an injector. High pressure vapor is extracted from the turbine and directed to the injector. The organic fluid from the condenser which enters the injector is pressurized and heated. The results indicate that the regenerative ORC with injector has a higher thermal efficiency than the basic ORC if the extraction pressure is lower than 390 kPa.

An ORC with reheat for solar applications was considered in the work of Price and Hassani [94]. They determined that the thermal efficiency of the cycle with reheat is only slightly higher than the case without reheat. A same conclusion was made by Mago et al. [52]. Additionally, the cost of the cycle with reheat is considered higher because of the need of a low- and high pressure expander and an extra heat exchanger. Therefore the reheat cycle is discarded as a viable alternative.

Another possibility is combining ORCs in a cascade. Each ORC is a separate stage. In contrast to the basic cycle, the condenser of the upper stage acts as the evaporator of the lower stage. By optimizing the working fluid of each stage, the thermal efficiency can be increased [95]. The heat input however, is determined exclusively by the upper stage.

3.9. Overview of challenges related to advanced ORC architectures

From the examined scientific literature above, some general challenges for each of the cycles architectures are compiled and given in Table 3. These highlight potential knowledge gaps where additional development and research is needed. Besides the listed challenges there is a general lack of experimental validation, which is tackled in the next section.

4. Prototypes and commercial installations

An overview of adaptations to the classical subcritical ORC by ORC manufacturers is given in Table 4. It is noteworthy that they all have their origin in low-temperature geothermal applications. Furthermore, the table suggests that new and complex cycle adaptations are, in first instance, only cost-effective for large installations. For large scale systems a small increase in efficiency already results in a significant increase in power output. Prototypes of three promising technologies were constructed: the TC, the MP and the TLC. In contrast to the TC or TLC, the MP [96] differs significantly in component layout from the basic ORC. Two manufacturers, namely Turboden [97] and TAS [98], invested in the development of transcritical cycles. Unalike TAS, the Turboden installation is an experimental prototype to assess the plant's design criteria and thermodynamic performance. Turboden expects the

Table 4
Adaptations to the classical subcritical ORC by commercial manufacturers.

Manufacturer	Installation	Cycle	Technical characteristics
TAS	Neal Hot Springs [98] (Oregon, USA)	TC	Geothermal brine at 138 °C, working fluid: R134a, net power output: 29.7 MWe
Ormat[a]	Ormesa I project [96] (California, USA)	MP	Geothermal brine at 147 °C, 26 units in 3 level cascade, total power output: 24 MWe
Energent	Coso [99] (California, USA)	TLC	Geothermal brine at 112 °C, total power output: 1 MWe
Turboden	Livorno [97] (Tuscany, Italy)	TC	Geothermal brine at 150 °C, total power output: 500 kWe

[a] Ormat has among others also MP type cycles in California, USA and Stillwater, USA [95].

Table 5
Overview of experimental data about advanced ORC architectures.

Ref.	Cycle	Topic
[101]	ZM	Heat transfer characteristics of siloxane mixtures
[102]	ZM	Determination pinch point and maximum temperature difference
[103]	ZM	On site measurements of subcritical ORC with R245fa and R245fa/R152a
[104]	ZM	Comparison R245fa and R245fa/R601a for ORC with scroll expander
[100]	TLC	Experiments on screw expanders in the range 5–850 kW
[105]	RC	Comparison of ORC with and without recuperator
[106]	RC	Onsite results for ORC with recuperator in solar applications
[107,108]	TC	Heat transfer in evaporator

plant to be 10–15% more efficient than currently available commercial technology.

The main challenge of designing a TLC is the availability of two-phase expanders. Energent [99] developed and patented the Variable Phase Turbine (VPT). The VPT can also be used in conditions where the working fluid is partially evaporated or even superheated. The VPT consists out of fixed nozzles and an axial impulse turbine. The inlet to the nozzle can be liquid, two-phase, supercritical or superheated vapor. The two-phase nozzle efficiency is claimed to be between 90% and 97%, while the rotor efficiency is between 78% and 85%. An alternative for accomplishing two-phase expansion is the use of volumetric machines. Especially the screw expander technology looks promising. Smith et al. [100] report that expander isentropic efficiencies of 70% and more are attainable for screw expanders.

Besides prototypes constructed by ORC manufacturers, there is limited experimental data available from open literature. An overview is given in Table 5. The publications are mainly focused on the subcritical ORC with recuperator, the trilateral cycle, the subcritical ORC with zeotropic mixtures and transcritical cycles.

Experiments on zeotropic mixtures focus on two major research questions: the effect on the heat transfer characteristics and the performance in real life setups. The first is addressed by Weith et al. [101] who analyzed the heat transfer characteristics of siloxane mixtures during evaporation. They found heat transfer degradations up to 46% compared to the assumed ideal values from linear interpolation. For R245fa/R365mfc, the degradation is even more severe. Wu et al. [102] investigated the pinch points and maximum temperature differences in a horizontal tube-in-tube evaporator for the mixtures R290/R600 (mass fraction: 0.15/0.85) and R245fa/R152a (mass fraction: 0.6/0.4). They demonstrate that the simplified models, where the apparent heat capacity is assumed to change linearly between saturated liquid and saturated vapor state, are insufficient to accurately predict the pinch point.

Wang et al. [103] addressed the topic of the overall cycle performance, by performing an onsite experimental study of a low-temperature solar subcritical ORC. The pure fluid R245fa was compared to the zeotropic mixtures R245fa/R152a (mass fraction: 0.9/0.1) and R245fa/R152a (mass fraction: 0.7/0.3). The resulting overall cycle efficiency was respectively 0.88%, 0.92% and 1.28%. Li et al. [104] made an experimental comparison between R245fa and R245fa/R601a (mass fraction: 0.72/0.28) for ORCs using a scroll expander. Their results confirm the better match with the heat source profile when using zeotropic mixtures as working fluid.

A difficulty with experimental studies, when comparing different thermodynamic cycles, is that the working fluids should be compared under their respective optimal conditions. Firstly, the components design (especially the expander) should be tuned for the specific working fluid. Additionally, the working fluids must be compared under optimal operating parameters.

The TLC with a screw expander as expansion device is extensively studied in the experimental work of Smith et al. [100]. Three different working fluids, varying rotor profiles and power outputs between 5 and 850 kW were investigated. The relatively large pressure drop at the inlet, associated with the initial filling between rotor and casing, was identified as a main factor contributing to the poor results of previous studies. They conclude that adiabatic efficiencies of 70% are possible at outputs of only 25 kW. Multi-megawatt machines are feasible with efficiencies of more than 80%.

Experiments which compared the ORC versus the ORC with recuperator were performed by Li et al. [105]. Water of 130 °C is fed to the ORC. The working fluid is R123 and passes through a single stage axial flow turbine. This setup gave a thermal efficiency of 7.98% and 6.15% for respectively the ORC with and without recuperator. Confirming the expected results of a higher thermal efficiency for an ORC with recuperator. Wang et al. [106] describe experiments for a solar ORC with recuperator. With constant working fluid mass flow rate, the recuperator did not improve the thermal efficiency of the system. To the contrary, the preheating caused the collector inlet temperature to increase, which led to lower collector efficiencies and ultimately, lower overall cycle efficiencies. However, when changing the working fluid mass flow rate, improvements in the overall system efficiencies are reported. This result confirms the importance of comparing cycle architectures under optimal operating and design conditions.

To the authors' knowledge no experimental data of a full transcritical cycle are available in literature. Bliem et al. [107,108] published some data about supercritical vapor generators working with pure isobutane and a butane/hexane mixture (mass fraction: 0.95/0.05). However, the developed computer code, HTRI (Heat Transfer Research, Inc.), is proprietary and no data about heat transfer correlations are shared. Furthermore, as the authors themselves note, the results are limited and insufficient to demonstrate the total system performance.

In contrast, there are several works which provide experimental results on CO_2 supercritical cycles. However these fall out of the scope of this article.

5. Conclusions

In this review article, the performance potential of cycle modifications to the basic ORC was illustrated. The focus is on waste heat recovery applications. The cycle configurations of interest are identified as:

- Transcritical cycles (TC)
- Trilateral cycles (TLC)
- Cycles with zeotropic mixtures as working fluids (ZM)
- Cycles with multiple evaporation pressures (MP)
- Organic flash cycles (OFC)
- Addition of a recuperator (RC)
- Regenerative cycle with turbine bleeding (RG)
- Cycle with vapor injector
- Cascade cycles
- Cycle with reheaters

These cycles were critically discussed based on the available literature. Future developments and potential knowledge gaps where identified. Some general challenges can be stated. Firstly, there is the difficulty in assessing the additional complexity of the system. Only for the transcritical cycle assessments are made based on techno-economic considerations. A further challenge is coping with the various boundary conditions used in literature, which makes a fair comparison difficult. Therefore special attention has been paid to clearly state the boundary conditions. Also the lack of experimental data has been revealed. Only for ORCs with zeotropic mixtures as working fluids, triangular cycles and cycles with recuperators some system validation results are available.

Acknowledgments

The results presented in this paper have been obtained within the frame of the IWT SBO-10006 project The Next Generation organic Rankine cycles (www.orcnext.be), funded by the Institute for the Promotion and Innovation by Science and Technology in Flanders. This financial support is gratefully acknowledged.

References

[1] Quoilin S, Broek MVD, Declaye S, Dewallef P, Lemort V. Techno-economic survey of Organic Rankine Cycle (ORC) systems. Renew Sustain Energy Rev 2013;22:168–86.
[2] Tchanche BF, Lambrinos G, Frangoudakis A, Papadakis G. Low-grade heat conversion into power using organic Rankine cycles – a review of various applications. Renew Sustain Energy Rev 2011;15:3963–79.
[3] Bronicki L. Short review of the long history of ORC power systems. ORC2013. Rotterdam; 2013.
[4] LIFE10/ENV/IT/000397. EU paper: ORC waste heat recovery in European energy intensive industries (Annex 4.2.II Paper EU). European Union; 2013.
[5] Hung TC, Wang SK, Kuo CH, Pei BS, Tsai KF. A study of organic working fluids on system efficiency of an ORC using low-grade energy sources. Energy 2010;35:1403–11.
[6] Lai NA, Wendland M, Fischer J. Working fluids for high-temperature organic Rankine cycles. Energy 2011;36:199–211.
[7] Liu B-T, Chien K-H, Wang C-C. Effect of working fluids on organic Rankine cycle for waste heat recovery. Energy 2004;29:1207–17.
[8] Rayegan R, Tao YX. A procedure to select working fluids for solar Organic Rankine Cycles (ORCs). Renew Energy 2011;36:659–70.
[9] Saleh B, Koglbauer G, Wendland M, Fischer J. Working fluids for low-temperature organic Rankine cycles. Energy 2007;32:1210–21.
[10] Zyhowski G, Brown A. Low global warming fluids for replacement of HFC-245fa and HFC-134a in ORC applications. In: Proceedings of ORC 2011; 2011.
[11] Angelino G, Gaia M, Macchi E. A review of the Italian activity in the field of Organic Rankine Cycles. In: Proceedings of international VDI seminar on ORC HP technology working fluids problems, Zurich, VBD Berichte; September 1984, vol. 539. p. 465–82.
[12] Cayer E, Galanis N, Nesreddine H. Parametric study and optimization of a transcritical power cycle using a low temperature source. Appl Energy 2010;87:1349–57.
[13] Lecompte S, Huisseune H, van den Broek M, De Schampheleire S, De Paepe M. Part load based thermo-economic optimization of the Organic Rankine Cycle (ORC) applied to a combined heat and power (CHP) system. Appl Energy 2013;111:871–81.
[14] Lecompte S, Lemmens S, Verbruggen A, Van den Broek M, De Paepe M. Thermo-economic comparison of advanced Organic Rankine Cycles. In: Proceedings of the international conference on applied energy; 2014.
[15] Lecompte S, Lazova M, Van den Broek M, De Paepe M. Multi-objective optimization of a low-temperature transcritical organic Rankine Cycle for waste heat recovery. In: Proceedings of 10th International Conference on Heat Transfer, Fluid Mechanics and Thermodynamics (HEFAT). Orlando, Florida; 2014. p. 6.
[16] Lecompte S, Van den Broek M, De Paepe M. Optimal sizing of heat exchangers for Organic Rankine Cycles (ORC) based on thermo-economics. In: Proceedings of 15th international heat transfer conference. Kyoto, Japan; 2014. p. 14.
[17] Wang J, Yan Z, Wang M, Li M, Dai Y. Multi-objective optimization of an organic Rankine cycle (ORC) for low grade waste heat recovery using evolutionary algorithm. Energy Convers Manag 2013;71:146–58.
[18] Wang ZQ, Zhou NJ, Guo J, Wang XY. Fluid selection and parametric optimization of organic Rankine cycle using low temperature waste heat. Energy 2012;40:107–15.
[19] Sauret E, Rowlands AS. Candidate radial-inflow turbines and high-density working fluids for geothermal power systems. Energy 2011;36:4460–7.
[20] Lemort V, Quoilin S, Cuevas C, Lebrun J. Testing and modeling a scroll expander integrated into an Organic Rankine Cycle. Appl Therm Eng 2009;29:3094–102.
[21] Cho S-Y, Cho C-H, Ahn K-Y, Lee YD. A study of the optimal operating conditions in the organic Rankine cycle using a turbo-expander for fluctuations of the available thermal energy. Energy 2014;64:900–11.
[22] Kang SH. Design and experimental study of ORC (organic Rankine cycle) and radial turbine using R245fa working fluid. Energy 2012;41:514–24.
[23] Casati E, Vitale S, Pini M, Persico G, Colonna P. Centrifugal turbines for mini-organic rankine cycle power systems. J Eng Gas Turbines Power 2014;136 122607-.
[24] Hou G, Bi S, Lin M, Zhang J, Xu J. Minimum variance control of organic Rankine cycle based waste heat recovery. Energy Convers Manag 2014;86:576–86.
[25] Zhang J, Zhou Y, Wang R, Xu J, Fang F. Modeling and constrained multi-variable predictive control for ORC (Organic Rankine Cycle) based waste heat energy conversion systems. Energy 2014;66:128–38.
[26] Quoilin S, Aumann R, Grill A, Schuster A, Lemort V, Spliethoff H. Dynamic modeling and optimal control strategy of waste heat recovery Organic Rankine Cycles. Appl Energy 2011;88:2183–90.
[27] Sapali SN. Refrigeration and air conditioning: PHI learning; 2009.
[28] Tchanche BF, Pétrissans M, Papadakis G. Heat resources and organic Rankine cycle machines. Renew Sustain Energy Rev 2014;39:1185–99.
[29] Ziviani D, Beyene A, Venturini M. Advances and challenges in ORC systems modeling for low grade thermal energy recovery. Appl Energy 2014;121:79–95.
[30] Bendig M, Maréchal F, Favrat D Defining. "Waste Heat" for industrial processes. Appl Therm Eng 2013;61:134–42.
[31] Meinel D, Wieland C, Spliethoff H. Effect and comparison of different working fluids on a two-stage organic rankine cycle (ORC) concept. Appl Therm Eng 2014;63:246–53.
[32] Maraver D, Royo J, Lemort V, Quoilin S. Systematic optimization of subcritical and transcritical organic Rankine cycles (ORCs) constrained by technical parameters in multiple applications. Appl Energy 2014;117:11–29.
[33] Wang C, He B, Sun S, Wu Y, Yan N, Yan L, et al. Application of a low pressure economizer for waste heat recovery from the exhaust flue gas in a 600 MW power plant. Energy 2012;48:196–202.
[34] Larjola J. Electricity from industrial waste heat using high-speed organic Rankine cycle (ORC). Int J Prod Econ 1995;41:227–35.
[35] Durmayaz A, Sogut OS, Sahin B, Yavuz H. Optimization of thermal systems based on finite-time thermodynamics and thermoeconomics. Prog Energy Combust Sci 2004;30:42.
[36] Öhman H, Lundqvist P. Comparison and analysis of performance using Low Temperature Power Cycles. Appl Therm Eng 2013;52:160–9.
[37] Crook AW. Profiting from low-grade heat. The Watt Committee on energy report: Institution of Electrical Engineers; 1994.
[38] Quoilin S, Lemort V. Technological and economical survey of Organic Rankine Cycle systems. In: Proceedings of the European conference on economics and management of energy in industry; 2009.
[39] Kotas TJ. The exergy method of thermal plant analysis. Malabar, Florida: Krieger; 1995.
[40] DiPippo R. Second Law assessment of binary plants generating power from low-temperature geothermal fluids. Geothermics 2004;33:565–86.
[41] Ho T, Mao SS, Greif R. Comparison of the Organic Flash Cycle (OFC) to other advanced vapor cycles for intermediate and high temperature waste heat reclamation and solar thermal energy. Energy 2012;42:213–23.
[42] Lecompte S, Ameel B, Ziviani D, van den Broek M, De Paepe M. Exergy analysis of zeotropic mixtures as working fluids in Organic Rankine Cycles. Energy Convers Manag 2014;85:727–39.

[43] Long R, Bao YJ, Huang XM, Liu W. Exergy analysis and working fluid selection of organic Rankine cycle for low grade waste heat recovery. Energy 2014;73:475–83.
[44] Quoilin S, Declaye S, Tchanche BF, Lemort V. Thermo-economic optimization of waste heat recovery Organic Rankine Cycles. Appl Therm Eng 2011;31:2885–93.
[45] Woudstra N, Woudstra T, Pirone A, Stelt TVD. Thermodynamic evaluation of combined cycle plants. Energy Convers Manag 2010;51:1099–110.
[46] Mago PJ, Srinivasan KK, Chamra LM, Somayaji C. An examination of exergy destruction in organic Rankine cycles. Int J Energy Res 2008;32:926–38.
[47] Shengjun Z, Huaixin W, Tao G. Performance comparison and parametric optimization of subcritical Organic Rankine Cycle (ORC) and transcritical power cycle system for low-temperature geothermal power generation. Appl Energy 2011;88:2740–54.
[48] Chen H, Goswami DY, Stefanakos EK. A review of thermodynamic cycles and working fluids for the conversion of low-grade heat. Renew Sustain Energy Rev 2010;14:3059–67.
[49] Aljundi IH. Effect of dry hydrocarbons and critical point temperature on the efficiencies of organic Rankine cycle. Renew Energy 2011;36:1196–202.
[50] Dai Y, Wang J, Gao L. Parametric optimization and comparative study of organic Rankine cycle (ORC) for low grade waste heat recovery. Energy Convers Manag 2009;50:576–82.
[51] Li W, Feng X, Yu LJ, Xu J. Effects of evaporating temperature and internal heat exchanger on organic Rankine cycle. Appl Therm Eng 2011;31:4014–23.
[52] Mago PJ, Chamra LM, Srinivasan K, Somayaji C. An examination of regenerative organic Rankine cycles using dry fluids. Appl Therm Eng 2008;28:998–1007.
[53] Desai NB, Bandyopadhyay S. Process integration of organic Rankine cycle. Energy 2009;34:1674–86.
[54] Pei G, Li J, Ji J. Analysis of low temperature solar thermal electric generation using regenerative Organic Rankine Cycle. Appl Therm Eng 2010;30:998–1004.
[55] Yari M, Mahmoudi SMS. A thermodynamic study of waste heat recovery from GT-MHR using organic Rankine cycles. Heat Mass Transf 2011;47:181–96.
[56] DiPippo R. Geothermal power plants: principles, applications, and case studies; 2005.
[57] Kehlhofer R, Hannemann F, Stirnimann F, Rukes B. Combined cycle gas en steam turbine power plants. Oklahoma, USA: Pennwell; 2009.
[58] Ho T, Mao SS, Greif R. Increased power production through enhancements to the Organic Flash Cycle (OFC). Energy 2012;45:686–95.
[59] Edrisi BH, Michaelides EE. Effect of the working fluid on the optimum work of binary-flashing geothermal power plants. Energy 2013;50:389–94.
[60] Yamada N, Mohamad MNA, Kien TT. Study on thermal efficiency of low- to medium-temperature organic Rankine cycles using HFO−1234yf. Renew Energy 2012;41:368–75.
[61] Schuster A, Karellas S, Aumann R. Efficiency optimization potential in supercritical Organic Rankine Cycles. Energy 2010;35:1033–9.
[62] Fischer J. Comparison of trilateral cycles and organic Rankine cycles. Energy 2011;36:6208–19.
[63] DiPippo R. Ideal thermal efficiency for geothermal binary plants. Geothermics 2007;36:276–85.
[64] Lai NA, Fischer J. Efficiencies of power flash cycles. Energy 2012;44:1017–27.
[65] Zamfirescu C, Dincer I. Thermodynamic analysis of a novel ammonia water trilateral Rankine cycle. Thermochim Acta 2008;477:7–15.
[66] Kalina AI, Leibowitz HM. System design and experimental development of the Kalina Cycle technology. In: Proceedings of industrial energy technology conference; 1987.
[67] Lu XL, Watson A, Deans J. Analysis of the thermodynamic performance of Kalina Cycle System 11 (KCS11) for geothermal power plant-comparison with Kawerau Ormat binary plant. In: Proceedings of the ASME 2009 3rd international conference of energy sustainability; 2009.
[68] Kalina AI. Method and apparatus for implementing a thermodynamic cycle using a fluid of changing concentration; 1986.
[69] Colonna P. Properties of fluid mixtures for thermodynamic cycles applications. Mech. Eng. Dept. Stanford University; 1995.
[70] Wong DSH, Sandler SI. A theoretically correct mixing rule for cubic equations of state. AIChE J 1992;38:671–80.
[71] Angelino G, Colonna P. Multicomponent working fluids for Organic Rankine Cycles (ORCs). Energy 1998;23:449–63.
[72] Heberle F, Preißinger M, Brüggemann D. Zeotropic mixtures as working fluids in Organic Rankine Cycles for low-enthalpy geothermal resources. Renew Energy 2012;37:364–70.
[73] Chys M, van den Broek M, Vanslambrouck B, Paepe MD. Potential of zeotropic mixtures as working fluids in organic Rankine cycles. Energy 2012;44:623–32.
[74] Wang XD, Zhao L. Analysis of zeotropic mixtures used in low-temperature solar Rankine cycles for power generation. Sol Energy 2009;83:605–13.
[75] Piwowarski M. Optimization of steam cycles with respect to supercritical parameters. Pol Marit Res 2009;1:45–51.
[76] Kauf F. Determination of the optimum high pressure for transcritical CO_2-refrigeration cycles. Int J Therm Sci 1999;38:325–30.
[77] Angelino G, Invernizzi C. Supercritical heat pumps. Int J Refrigeration 1994;17:12.
[78] Feher EG. The supercritical thermodynamic power cycle. Energy Convers Manag 1968;8:5.
[79] Dekhtiarev VL. On designing a large, highly economical carbon dioxide power installation. Elecrtichenskie Stantski 1962;5:6.
[80] Angelino G. Perspectives for the liquid phase compression gas turbine. ASME Paper no. 66-GT-111; 1966.
[81] Baik Y-J, Kim M, Chang KC, Kim SJ. Power-based performance comparison between carbon dioxide and R125 transcritical cycles for a low-grade heat source. Appl Energy 2011;88:892–8.
[82] Astolfi M, Romano MC, Bombarda P, Macchi E. Binary ORC (organic Rankine cycles) power plants for the exploitation of medium–low temperature geothermal sources – Part A: thermodynamic optimization. Energy 2014;66:423–34.
[83] Vetter C, Wiemer H-J, Kuhn D. Comparison of sub- and supercritical Organic Rankine Cycles for power generation from low-temperature low-enthalpy geothermal wells, considering specific net power output and efficiency. Appl Therm Eng 2013;51:871–9.
[84] Karellas S, Schuster A, Leontaritis A-D. Influence of supercritical ORC parameters on plate heat exchanger design. Appl Therm Eng 2012;33–34:70–6.
[85] Jackson JD, Hall WB, Fewster J, Watson A, Watts MJ. Heat transfer to supercritical pressure fluids. Design report 34: U.K.A.E.A.; 1975.
[86] Nag PK. Power plant Engineering. New Delhi, India: Tata McGraw-Hill; 2008.
[87] Kanoglu M. Exergy analysis of a dual-level binary geothermal power plant. Geothermics 2002;31:709–24.
[88] Stijepovic MZ, Papadopoulos AI, Linke P, Grujic AS, Seferlis P. An exergy composite curves approach for the design of optimum multi-pressure organic Rankine cycle processes. Energy 2014;69:285–98.
[89] Lee W-Y, Kim S-S. The maximum power from a finite reservoir for a Lorentz cycle. Energy 1992;17:275–81.
[90] Gnutek Z, Bryszewska-Mazurek A. The thermodynamic analysis of multicycle ORC engine. Energy 2001;26:1075–82.
[91] Franco A, Villani M. Optimal design of binary cycle power plants for water-dominated, medium-temperature geothermal fields. Geothermics 2009;38:379–91.
[92] Becquin G, Freund S. Comparative performance of advanced power cycles for low-temperature heat sources. In: Proceedings of ECOS; 2012.
[93] Xu R-J, He Y-L. A vapor injector-based novel regenerative organic Rankine cycle. Appl Therm Eng 2011;31:1238–43.
[94] Price H, Hassani V. Modular through power plant cycle and system analysis. Golden, Colorado, USA: National Renewable Energy Laboratory; 2002. p. 118.
[95] Kosmadakis G, Manolakos D, Kyritsis S, Papadakis G. Economic assessment of a two-stage solar organic Rankine cycle for reverse osmosis desalination. Renew Energy 2009;34:1579–86.
[96] Bronicki L. Innovative geothermal power plants fifteen years of experience. Ormat Geothermal Division; 1995. p. 4.
[97] Turboden. The Company and the Geothermal Applications; 2012.
[98] TAS. U.S. Geothermal 22 MW Neal hot springs geothermal power plant TAS; 2013.
[99] Energent. Construction and startup of low temperature geothermal power plants; 2011.
[100] Smith IK, Stosic N, Aldis CA. Development of the trilateral flash cycle system= Part 3: the design of high-efficiency two-phase screw expanders. Proc Inst Mech Eng, Part A: J Power Energy 1996;210:75–93.
[101] Weith T, Heberle F, Preißinger M, Brüggemann D. Performance of siloxane mixtures in a high-temperature organic rankine cycle considering the heat transfer characteristics during evaporation. Energies 2014;7:5548–65.
[102] Wu W, Zhao L, Ho T. Experimental investigation on pinch points and maximum temperature differences in a horizontal tube-in-tube evaporator using zeotropic refrigerants. Energy Convers Manag 2012;56:22–31.
[103] Wang JL, Zhao L, Wang XD. A comparative study of pure and zeotropic mixtures in low-temperature solar Rankine cycle. Appl Energy 2010;87:3366–3373.
[104] Li T, Zhu J, Fu W, Hu K. Experimental comparison of R245fa and R245fa/R601a for organic Rankine cycle using scroll expander. Int J Energy Res 2014;39:202–14.
[105] Li M, Wang J, He W, Gao L, Wang B, Ma S, et al. Construction and preliminary test of a low-temperature regenerative Organic Rankine Cycle (ORC) using R123. Renew Energy 2013;57:216–22.
[106] Wang JL, Zhao L, Wang XD. An experimental study on the recuperative low temperature solar Rankine cycle using R245fa. Appl Energy 2012;94:34–40.
[107] Bliem CJ, Mines GL. Initial results for supercritical cycle experiments using pure and mixed-hydrocarbon working fluids. Geotherm Resour Counc Trans 1984;8:6.
[108] Bliem CJ, Demuth OJ, Mines GL, Swank WD. Vaporization at supercritical pressures and counterflow condensing of pure and mixed-hydrocarbon working fluids for geothermal power plants. In: Proceedings of the intersociety energy conversion engineering conference. San Diego, USA. p. 5.